Adhesion Property and Morphology of Styrene Triblock/Diblock Copolymer Blends

Mariko Sasaki,[1] Manabu Adachi,[2] Yosuke Kato,[2] Syuji Fujii,[2] Yoshinobu Nakamura,[2,3] Yoshiaki Urahama,[4] Shinichi Sakurai[5]

[1]Nitto Analytical Techno-Center Co. Ltd., Nakahara-cho, Toyohashi-shi, Aichi 441-3194, Japan
[2]Department of Applied Chemistry, Osaka Institute of Technology, Asahi-ku, Osaka 535-8585, Japan
[3]Nanomaterials Microdevices Research Center, Osaka Institute of Technology, Asahi-ku, Osaka 535-8585, Japan
[4]Japan Adhesive Tape Manufacturers Association, Chiyoda-ku, Tokyo 101-0047, Japan
[5]Department of Macromolecular Science and Engineering, Graduate School of Science and Technology, Kyoto Institute of Technology, Matsugasaki, Sakyo-ku, Kyoto 606-8585, Japan

ABSTRACT: Relationship between adhesion properties and phase structures of styrene triblock and diblock copolymer blends was investigated in detail. For this purpose, polystyrene-*block*-polyisoprene-*block*-polystyrene triblock and polystyrene-*block*-polyisoprene diblock copolymers were used and the diblock content was varied from 0 to 100 wt %. All blends formed the sea-island structure in which spherical polystyrene domains were dispersed in polyisoprene matrix and mean domain size was $\sim$ 20 nm. The domain size was slightly affected by the diblock content. The fracture stress and strain measured by a tensile test decreased and the molecular mobility measured by a ^{1}H pulse nuclear magnetic resonance analysis increased with an increase of diblock content. The tack as adhesion property increased with an increase of diblock content below 70 wt %, then decreased over 70 wt %. The cohesive strength decreased and the interfacial adhesion increased with an increase of diblock content. The tack increases by the development of cohesive strength and interfacial adhesion. Therefore, the tack showed the maximum at the optimum contribution balance between cohesive strength and interfacial adhesion. © 2010 Wiley Periodicals, Inc. J Appl Polym Sci 118: 1766–1773, 2010

Key words: adhesion; adhesives; block copolymers; morphology; SAXS

INTRODUCTION

Styrene block copolymers, such as polystyrene (PS)-*block*-polyisoprene (PI) diblock copolymer (SI) and PS-*block*-PI-*block*-PS triblock copolymer (SIS) are known to form various unique nanosized phase structures.[1] Effects of polymer composition, content, casting solvent, and temperature on phase structure have been investigated[2–12] and sea-island structure, cylinder-like, and lamellar-like structures have been reported. The block copolymers with relatively low molecular weights (tens of thousands) are usually used for the investigations of phase structures because they form clearer phase structures comparing with those with higher molecular weights (hundreds of thousands). However, they are not suitable for practical use because of their low cohesive strength. Those with molecular weights of hundreds of thousands show enough cohesive strength and they are used as "thermoplastic elastomer". However, studies on effects of the phase structure on the mechanical properties of the block copolymer with such higher molecular weight have been limited.

Recently, SIS with higher molecular weight is used as base polymer for pressure sensitive adhesive as an alternative material for chemically crosslinked rubber. For production of chemically crosslinked rubber-based pressure sensitive adhesives, organic solvents are required, whereas SIS-based adhesives can be produced just by hot-melt coating without any organic solvent. From the view point of green chemistry, the SIS-based adhesives are favorable and the SIS-based pressure sensitive adhesive tapes have found their applications as functional materials for surface protection etc.

In a series of our investigations,[13–15] we have been investigating the adhesion mechanism of pressure sensitive adhesive consisting of tackifier and SIS or an acrylic block copolymer as base polymers. It has been clarified that the nanosized phase separated structure of tackifier in SIS is important to show tackiness. Furthermore, the SIS has the potential to produce the higher performance adhesive by controlling the compatibility of the tackifier to PS and

Correspondence to: Y. Nakamura (nakamura@chem.oit.ac.jp).

TABLE I
Weight-Average Molecular Weights of SIS[a] and SI[b] Block Copolymers

Sample	M_w of SIS (M_w/M_n)	M_w of SI (M_w/M_n)	SI content (wt%)	PS content (wt%)
SI-0	220,000 (1.01)	–	0	15
SI-17	220,000 (1.01)	110,000 (1.01)	17	15
SI-50	250,000 (1.01)	125,000 (1.01)	50	16
SI-70	230,000 (1.01)	115,000 (1.01)	70	15
SI-100	–	110,000 (1.01)	100	15

SI contents and PS contents for SIS/SI blends used in this study are shown.
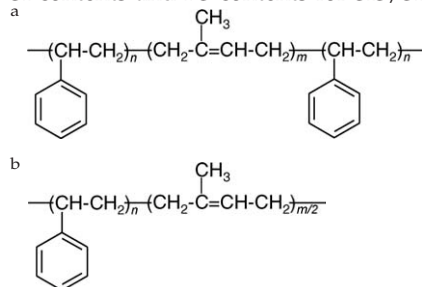
PI, because PS and PI have different solubility parameter values[16] as mentioned previously.[14]

In general, so-called "SIS" for the base polymer of pressure sensitive adhesive is blend of SIS and SI. The pure SIS is hard and show lower interfacial adhesion even with tackifier, because the molecular mobility of PI unit in SIS is strongly restricted by the PS unit. The PI unit in SI has higher degree of freedom than that in SIS. We previously used a commercially available SIS/SI blend (1/1, w/w).[13,14] Gibert et al.[17] and Roos and Creton[18] already investigated the viscoelastic and mechanical properties of SIS/SI blend.

In this study, the influences of SI addition on the molecular mobility and the adhesion properties of SIS/SI blend were investigated. The spin–spin relaxation time (T_2) measured by a ^{1}H pulse nuclear magnetic resonance analysis (NMR) shows the molecular mobility. Especially, the relationship between the molecular mobility and the interfacial adhesion was discussed. The influence of SI addition on the phase structure was also investigated by an atomic force microscopy (AFM) and a small-angle X-ray scattering (SAXS).

EXPERIMENTAL

Materials

Table I shows chemical structures and weight-average molecular weights (M_w) of SIS and SI block copolymers and SI contents and PS contents of the SIS/SI blends used in this study. The SI content was varied keeping a constant PS content of $\sim$ 15 wt %. The SIS/SI blends were kindly donated from Kraton JSR Elastomers K.K., Tokyo, Japan. The gel permea-

tion chromatography (GPC) measurements indicate the SIS and the SI are near-monodisperse. The polydispersibility indexes were near 1 (see Table I). The SIS and the SI started to decompose over 220°C confirmed by the thermo gravimetry and differential thermal analyses.

Reagent grade toluene was used as received from Sigma Aldrich Japan, Tokyo, Japan.

Sample preparation

The toluene solution of the SIS/SI blend was prepared at a solid content of 40 wt %. The solutions were cast on the PET sheet with a thickness of 38 μm. After toluene evaporation at room temperature, the cast film was heated at 100°C for 10 min *in vacuo*. The thickness of the SIS/SI blend film was about 50 μm, which was measured using a thickness indicator (Dial thickness gauge H-MT, Ozaki Mfg., Tokyo, Japan).

To prepare the thick sheet specimen, the toluene solutions were cast on the separator paper and the toluene was evaporated at room temperature for 1 week. The obtained sheet was heated at 100°C for 30 min *in vacuo* and pressed compressively at 100°C for 2 min with a pressure of 20 MPa. The thickness of the SIS/SI blend sheet was about 1 mm.

Mechanical properties

The sheet with a thickness of 1 mm prepared in the previous section was cut into rectangles (10 × 60 mm). The stress-strain curve was recorded using a tensile testing machine (AG-5KNIS, Shimadzu Corp.,

Kyoto, Japan) with a chuck distance of 30 mm and a tensile rate of 50 mm/min.

Peel strength

The SIS/SI film with PET sheet prepared in the previous section was cut in strip of 25 mm wide and then the strip was placed onto a stainless steel plate (SUS304BA, Nippon Tact, Tokyo, Japan) used as an adherend. The strip on the stainless steel was pressed using a 2-kg iron roller to develop good contact between the adhesive and the steel plate. Test specimens were subjected to five press cycles: the iron roller moved backward and forward as one press cycle. Some test specimens were further heated at 80°C for 2 h after five press cycles to improve the interfacial adhesion. 20–40 min after specimen preparation, the peel test was conducted.

The 180° peel strength was measured at a peel rate of 300 mm/min at room temperature using a tensile testing machine (AG-5KNIS, Shimadzu Corp., Kyoto, Japan) in accordance with JIS Z 0237 (Japanese Industrial Standards).[13–15]

Tack measurement

Tack[19] of the SIS/SI blend was measured using a probe tack tester (TE-6002, Tester Sangyo, Saitama, Japan) using a stainless steel (SUS 304) probe with 5 mm diameter at 23–25°C. The sample adhesive tape was attached on the weight, and the weight was set on the supporting board. When the supporting board declined and the probe lifted up the weight, the contact of probe and the sample adhesive tape started. In this apparatus, the probe is fixed. After a constant contact time, the peeling occurred when the supporting board elevated. The stress-displacement curve of the peeling process was recorded, and the tack was calculated from the maximum stress of the curve. The displacement rate of probe is 10 mm/s, the applied load by the weight is 1 N/mm^2 and the contact time is set in the range from 1 to 3000 s (standard contact time is 1 s).

Observations of phase structure and molecular mobility

AFM, SAXS, ^{1}H pulse NMR, and a dynamic mechanical analysis (DMA) were used to examine the phase structure and molecular mobility of the SIS/SI blends.

For an AFM measurement, the sample film of the SIS/SI blend was held using an electrical conductive pressure sensitive tape on a sample holder and the phase structure of the surface was observed using an AFM (SPM-9500J, Shimadzu Corp., Japan) by the tapping mode (phase image) in air atmosphere. A silicon probe with a spring constant of 42 N/m was used.

For a SAXS measurement, the SIS/SI blend film was cast from 5 wt % toluene solution, and the prepared film was annealed at 180°C for 6 h in nitrogen atmosphere. The SAXS measurements were conducted using a beamline (BL-9C) at the Photon Factory in the Research Organization for High Energy Accelerator, Tsukuba, Japan. The wavelength of incident X-rays, λ, was tuned at 0.154 nm. The details of the SAXS apparatus are available in literatures.[20] The imaging plate (250 × 200 mm^2), of actual pixel size 100 × 100 μm^2, was used as a two-dimensional detector. The typical exposure time was about 30 s. BAS2500 (Fuji Photo Film) was used for development of exposed 2D-SAXS images. The 2D-SAXS patterns were further converted to one-dimensional profile by conducting so-called circular average. No further correction such as a background subtraction was made on the 1D- and 2D-SAXS results.

^{1}H pulse NMR (JNM-MU25, JEOL, Tokyo, Japan) measurement was carried out by the Hahn echo method at 35°C with a sampling time of 4 ms in the same way with the previous studies.[13–15]

The dynamic viscoelastic properties were studied using a dynamic mechanical analyzer (DVA-200, ITK, Osaka, Japan) in a shear mode at 10 Hz frequency, heating rate of 6°C/min and 0.25% of applied strain as shown in our previous studies.[13–15] The measurements were conducted at temperatures ranging from −80 to 180°C.

RESULTS AND DISCUSSION

As shown in Table I, the PS content in the SIS, the SI and the SIS/SI blends was set constant at 15 wt %. Matsen and Bates[2] showed that the SI diblock copolymer with similar PS content with our system form the phase structure in which the spherical PS domains were dispersed in the PI matrix.

Figure 1 shows the stress-strain curves of the SIS/SI blends. The pure SIS showed the highest fracture stress and strain and the pure SI showed no stress. For the SIS/SI blends, both the fracture stress and strain decreased with an increase of the SI content. The SI in the SIS/SI blend significantly decreases a cohesive strength. The PS units in SIS restrict the mobility of PI unit strongly, and the PS domains in SIS act as pseudo cross-linking point. However, the reinforcement effect decreased with the SI content.
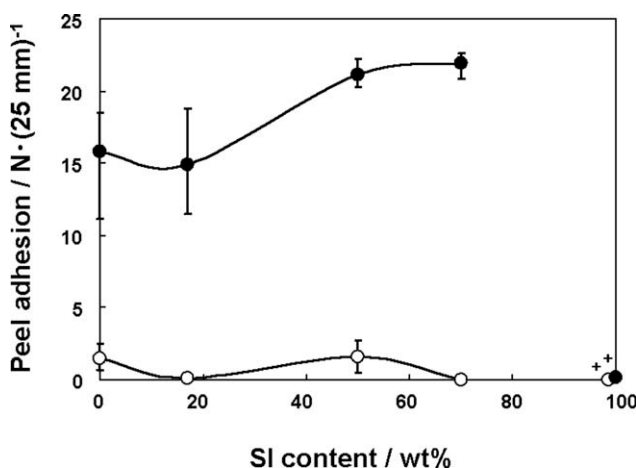
Figure 2 shows the relation between the peel strength and the SI content in the SIS/SI blend. For the specimens which were pressed five times at room temperature (○), the pure SIS showed low peel strength, and the peel strength never increased in the SI content range between 0 and 70 wt %. In the case of the adhesive with good molecular
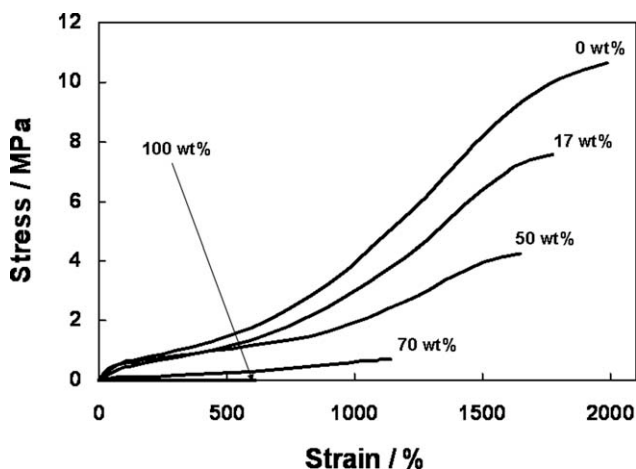
Figure 1 Stress-strain curves of SIS/SI blends with various SI content.

mobility, the adhesive molecules can move and interact with cohesive surface via van der Waals attraction, which leads to the significant interfacial adhesion. It seems that the sufficient interfacial adhesion was not achieved by the pressing at room temperature because of the lower molecular mobility of the PI unit. The failure mode was interfacial failure for all specimens except the pure SI. The pure SI showed the cohesive failure because of good interfacial adhesion and low cohesive strength of the adhesives. As clarified previously,[13,14] the addition of tackifier to SIS improves the molecular mobility.

For the specimens which were heated at 80°C after five times pressing to develop the interfacial adhesion (●), the sufficient peel strength was obtained and the value increased from 16 to 22 N·(25 mm)$^{-1}$ with an increase of the SI content. The adhesion strength should be influenced by two factors: the co-
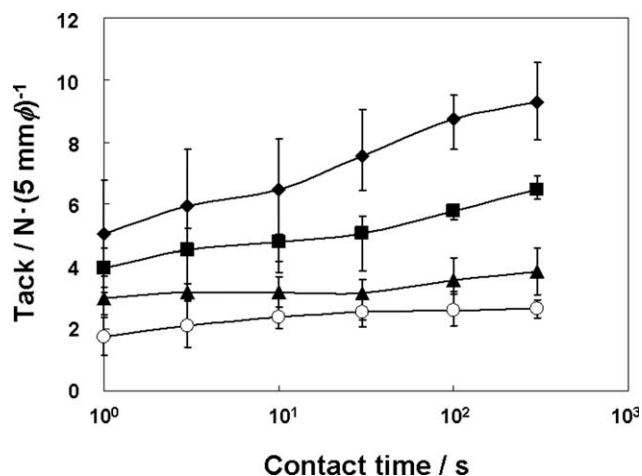
hesive strength of adhesive and the interfacial adhesion between adhesive and adherend. The result in Figure 1 demonstrated the cohesive strength of the SIS/SI blend decreased with an increase of the SI content. Therefore, the increase of peel strength with the SI content shown in Figure 2 should be caused by the improvement of interfacial adhesion. The pure SI showed no peel strength for both the only pressing and the further heated specimens. This was caused by low cohesive strength of the pure SI.

In this study, the specimen was heated at 80°C (below the glass transition temperature (T_g) of PS, about 100°C[21]) to avoid the deforming of the phase structure.

From the results shown above, it was found that the SI in the SIS/SI blend improves the interfacial adhesion. Next, the tack was measured. The peel strength was measured after sufficient interfacial contact, whereas the tack is measured after contact with lower load and shorter time. Therefore, the influence of interfacial adhesion seems to appear more significantly in the tack than in the peel strength.

Figure 3 shows the influences of the SI content in the SIS/SI blend and the contact time on the tack. The tack of the SIS/SI blend increased with an increase of the SI content, although that of the pure SI became lower than that of 70 wt % of SI content. The failure mode of the pure SI was the cohesive failure and that of others were the interfacial failure. This was caused by low cohesive strength of the pure SI. The tack gradually increased with the increase of the contact time. The SIS/SI blend with 70 wt % SI showed largest tack increase rate with the contact time. These results also indicate that the SI improves the interfacial adhesion.

Figure 4 shows the influence of the SI content in the SIS/SI blend on the tack measured after 1 s

Figure 2 Effect of SI content on the peel adhesion of SIS/SI blends. The test specimen was 5 times pressed with a 2 kg roller (○) and further heated (80°C, 2 h) after 5 times pressed (●). The failure modes were cohesive failure (+) and interfacial failure (no symbol).

Figure 3 Effect of contact time on the tack of SIS/SI blends with SI contents of 0 (○), 50 (▲), 70 (◆) and 100 wt % (■) measured by a probe tack test.
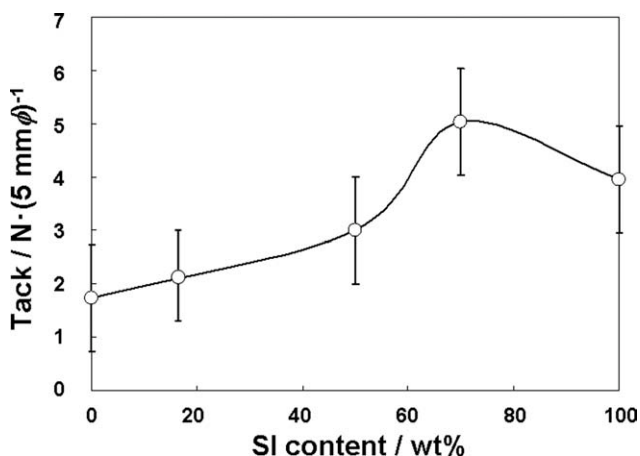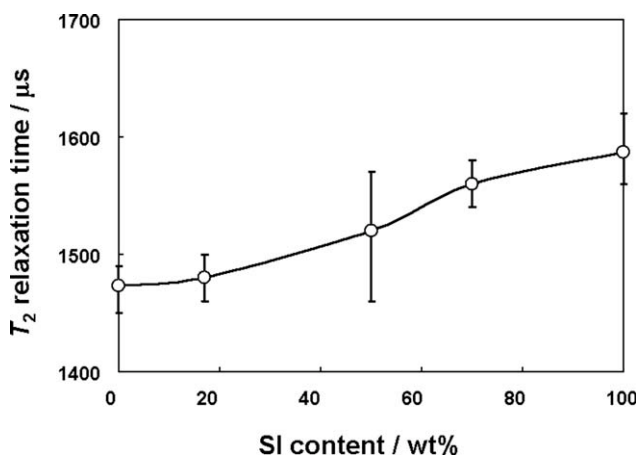
Figure 4 Effect of SI content on the tack of SIS/SI blends measured by a probe tack test. The contact time is 1 s.

contact time. It is clear that the tack showed the maximum value at the SI content of 70 wt %. This was caused by the contribution balance between the cohesive strength and the interfacial adhesion on the tack as mentioned above.

A ^{1}H pulse NMR measurement was carried out to investigate the influence of the SI content on the molecular mobility of the PI unit in the SIS/SI blend.

Figure 5 shows the T_2 relaxation time of the SIS/SI blends as a function of the SI content measured by a ^{1}H pulse NMR. There are two methods for a pulse NMR: the solid echo and the Hahn echo methods.[13–15] The solid echo method is suitable for clarifying the relative difference of molecular mobility in the phase separated polymer with hard and soft phases. On the other hand, the Hahn echo method is suitable for the measurement of molecular mobility of a soft material, such as elastomer with single phase or only soft phase in a phase separated polymer. In this study, the Hahn echo method was applied to characterize molecular mobility of contin-
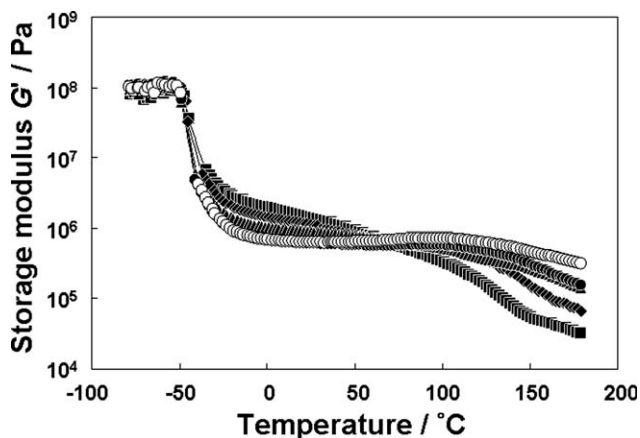
uous PI phase. The T_2 relaxation time increased with an increase of the SI content, which indicates the molecular mobility of PI increased by the addition of SI. The SI does not bridge two PS domains and the restriction of PI motion by the PS unit was reduced. This is the reason why the interfacial adhesion increased with the SI content. The T_2 relaxation time of pure PI (2 ms) was larger than that of PI unit in the pure SI (1.6 ms, see Fig. 5), which means that the molecular mobility of the PI unit is restricted by the neighboring PS unit even in the pure SI.

Figure 6 shows the temperature dependence of storage shear modulus (G') of the SIS/SI blends. The G' decreased drastically at about $-50°C$ for the all SIS/SI blends. This temperature accords well with the T_g of the PI unit. Above this temperature, the G' showed almost the same values (so-called the rubbery elastic plateau region) up to about 100°C in the case of the pure SIS. In the pure SIS, the molecular mobility of PI unit is restricted by the PS domains as pseudo closslinking points. In the rubbery elastic plateau, the temperature dependence of G' increased with an increase of the SI content. The G' decreased gradually above 100°C for the pure SIS, and the degree of decrease became more significant. This indicates that the T_g of the PS unit decreased with an increase of the SI content. These phenomena were caused by the restriction of PI unit mobility by the PS unit was weakened with an increase of the SI content.

Figure 7 shows the temperature dependence of loss tangent (tan δ) of the SIS/SI blends. The peaks at about $-50°C$ are based on the T_g of the PI unit, and were independent of the SI content. No clear peak based on the PS unit was observed for all the SIS/SI blends because the PS units form the dispersed phase. The tan δ value increased gradually above 50°C for the pure SIS, and it became more

Figure 5 Effect of SI content on the T_2 relaxation time of SIS/SI blends measured by a pulse ^{1}H NMR.

Figure 6 Storage modulus (G') of SIS/SI blends with SI contents of 0 (○), 17 (●), 50 (▲), 70 (◆), and 100 wt % (■) measured by a dynamic mechanical analysis. Measured frequency is 10 Hz.
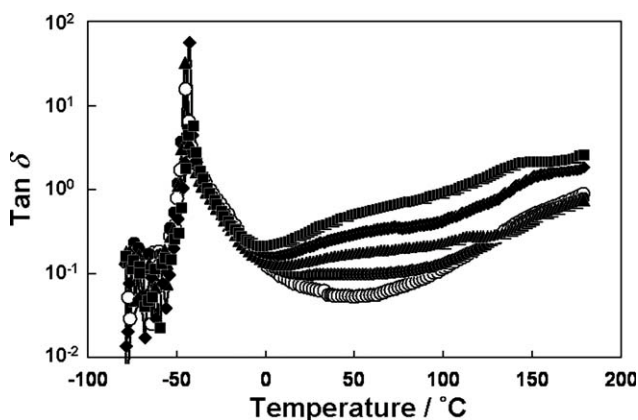
Figure 7 Loss tangent (Tan δ) of SIS/SI blends with SI contents of 0 (○), 17 (●), 50 (▲), 70 (◆), and 100 wt % (■) measured by a dynamic mechanical analysis. Measured frequency is 10 Hz.

significant with an increase of the SI content, and the new broad peak appeared at about 50°C for the SI contents of 70 (◆) and 100 wt % (■). These peaks are attributed to the SI, which possesses higher molecular mobility.

From the results above, it was found that the SI affected significantly on the mechanical and adhesion properties of the SIS/SI blend. Next, the influence of SI on the morphology of the SIS/SI blend was investigated.

Figure 8 shows the AFM images of the SIS/SI blends measured by the phase mode. The phase mode measures the relative hardness of specimen surface: the darker parts show the PS domains and the brighter parts show the PI matrix. In the pure SIS (a), the phase structure in which the PS domains

with about a diameter of 20 nm were dispersed in the PI matrix was clearly observed. The domain size seems to be largest in the SI content of 50 wt % (c) and smallest in the pure SI (e). To confirm this observation, the domain number in the AFM image was counted and the distance between PS domains was measured.

Figure 9 shows the domain number and the distance between PS domains observed in the SIS/SI blends. The domain number (counted in the 500 × 500 nm square of an AFM image) decreased with an increase of the SI content. The minimum value was at 50 wt %, and the domain number increased above 50 wt %. The distance between PS domains increased up to 50 wt % SI content and then decreased with an increase of the SI content. The AFM studies can observe only surface morphology. To confirm the inner morphology quantitatively, the SAXS experiments were carried out.

Figure 10 shows SAXS profiles (plots of logarithm of the scattering intensity, $I(q)$, as a function of the magnitude of the scattering vector, q, which is defined as $q = (4\pi/\lambda) \sin (\theta/2)$, where θ is the scattering angle. Three lattice scattering peaks appeared in the profile for the pure SIS. The relative ratio of the peak positions was expressed by $1 : \sqrt{2} : \sqrt{3}$. This result indicates that the phase structure in the pure SIS sample is such that spherical PS domains are ordered in a body-centered cubic (BCC) lattice embedded in the PI matrix.[22] The BCC lattice peaks were most broad for the SIS/SI blend with 50 wt % of the SI content, indicating that the regularity of the ordered-spherical domains is lowest among the samples examined in this study. In each SAXS profile, not only the lattice peaks, but also a broad peak due
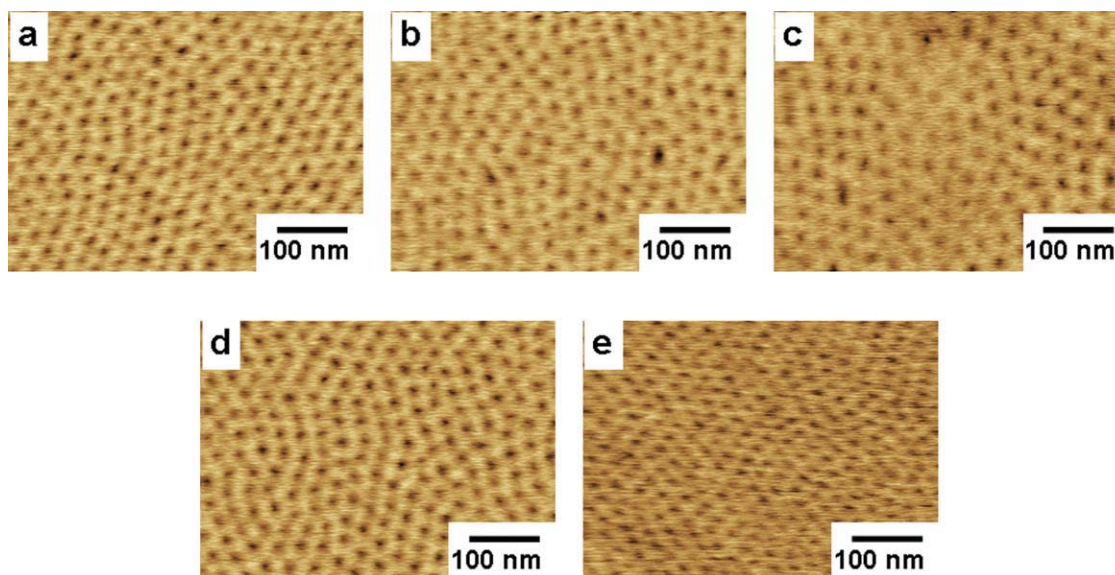
Figure 8 AFM images of SIS/SI blends with SI contents of (a) 0, (b) 17, (c) 50, (d) 70, and (e) 100 wt %. [Color figure can be viewed in the online issue, which is available at www.interscience.wiley.com.]
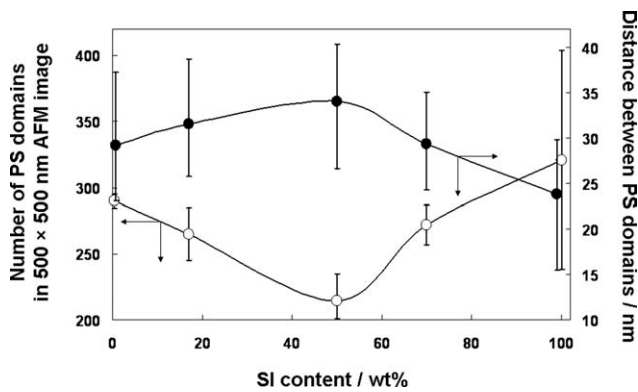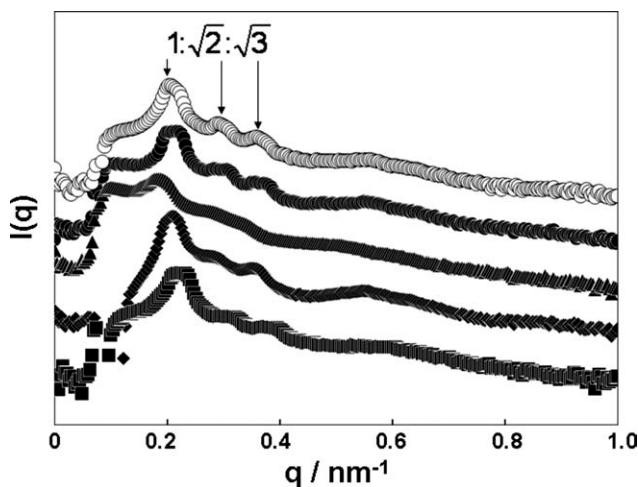
Figure 9 Effects of SI content on the number and the spacing of PS domains in SIS/SI blends measured using AFM images shown in Figure 8.
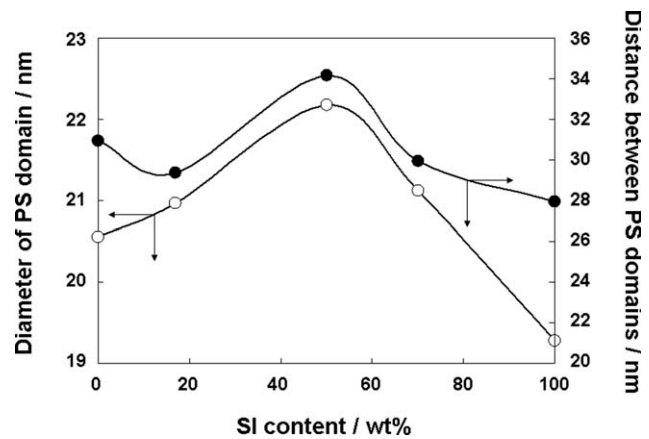
to the particle scattering factor appeared around $q = 0.5$–0.6 nm^{-1}. From the position of the particle scattering peak (q^*), it is possible to calculate the average radius of spheres as $R = 5.765 /q^*$.[23] Here, it should be noted that from the position of the first-order BCC lattice peak (q_1) the average spacing of the BCC {110} planes can be evaluated as $d_{110} = 2\pi/q_1$, and then the domain spacing (interdomain distance between the nearest neighbors) is to be as $(\sqrt{3}/\sqrt{2})^*d_{110}$.

Figure 11 shows the PS domain size and the distance between PS domains estimated by the SAXS results shown in Figure 10. At 50 wt % SI content, PS domain shows maximum diameter, which accord well with the result obtained from the AFM image shown in Figure 9.

Figure 12 shows the schematic views illustrating the influence of the SI content on the domain size in the SIS/SI blend. For the SIS (a), all the PI units are bridged between two PS domains or looped on the domain surface, and this structure strongly restrict
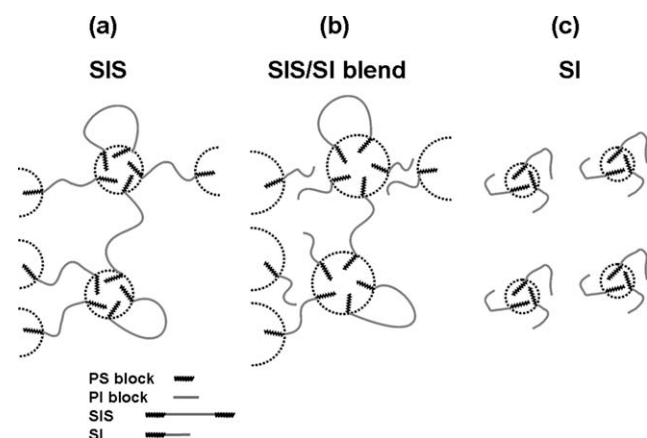

Figure 11 Effects of SI content on the diameter and the spacing of PS domains in SIS/SI blends measured by a small-angle X-ray scattering analysis.

the molecular mobility of the PS unit in the SIS. Therefore, the PI middle unit prevents the further agglomeration of PS unit. For the SIS/SI blend (b), the PS unit in the SI has higher degree of freedom than that in the SIS, and the amount of bridged PI unit between two PS domains decreased with an increase of the SI content. The PS units tend to agglomerate more easily with the increase of its degree of freedom, and the PS domain size increased gradually until the 50 wt % of the SI content (a → b). For the SI (c), the PI unit in the SI has also higher degree of freedom than that in the SIS. The PI unit with higher mobility tends to aggregate around the PS domain, and the concentration of PI increased at the near surface region. The PI-rich layer prevents to agglomerate the PS domains and the PS domain size decreased at the SI content above 50 wt % (b → c). These seem to be the reason why the PS domain size changed slightly and intricately dependent upon the SI content.

From the above results, it was concluded that the mechanical and the adhesion properties of the SIS/SI blend changed drastically depending on the SI

Figure 10 Small-angle X-ray scattering profiles of SIS/SI blend with SI contents of 0 (○), 17 (●), 50 (▲), 70 (◆), and 100 wt % (■).

Figure 12 Schematic views of phase structure for (a) SIS, (b) SIS/SI blend, and (c) SI.

content, whereas the phase structure changed slightly. In this study, the SIS/SI blend was cast from the toluene solution. It was already confirmed that toluene is the good solvent for both PS and PI.[14] The solvent also affected on the morphology of the SIS/SI blend, and it will be reported in our future article. The influence of the SI content on the adhesion property of the SIS/SI/tackifier system will be discussed in our next study.

CONCLUSIONS

The effects of the SI content in the SIS/SI blend on the adhesion properties and the phase structure of the SIS/SI blends were investigated. The following results were obtained.

(i) The SIS/SI blend showed the phase structure in which the spherical PS domains with a mean size of 20 nm were dispersed in the PI matrix. The PS domain size was dependent slightly on the SI content.

(ii) The mechanical and adhesion properties of the SIS/SI blend changed drastically with the SI content. The fracture stress and strain decreased, the temperature dependency of G' increased and the molecular mobility of the SIS/SI blend increased with an increase of the SI content.

(iii) The tack increased with an increase of the SI content below 70 wt %, then decreased over 70 wt %. The adhesion strength should be influenced by two factors: the cohesive strength of adhesive and the interfacial adhesion between adhesive and adherend. The cohesive strength decreased, whereas the interfacial adhesion increased with an increase of the SI content. Therefore, the tack showed the maximum value.

References

1. Molau, G. E. In Block Copolymers; Aggarwal, S. L., Ed.; Plenum Press: New York, 1970.
2. Matsen, M. W.; Bates, F. S. Macromolecules 1996, 29, 1091.
3. Sakurai, S.; Hashimoto, T.; Fetters, L. J. Macromolecules 1996, 29, 740.
4. Watanabe, H.; Sato, T.; Osaki, K. Macromolecules 2000, 33, 2545.
5. Hasegawa, H.; Hashimoto, T. Polymer 1992, 33, 475.
6. Hashimoto, T.; Fujimaru, M.; Kawai, H. Macromolecules 1980, 13, 1660.
7. Bang, J.; Jain, S.; Li, Z.; Lodge, T. P.; Pedersen, J. S.; Kesselman, E.; Talmon, Y. Macromolecules 2006, 39, 1199.
8. Sakurai, S.; Kota, T.; Isobe, D.; Okamoto, S.; Sakurai, K.; Ono, T.; Imaizumi, K.; Nomura, S. J Macromol Sci Phys 2004, 43, 1.
9. Sakurai, S.; Bando, H.; Yoshida, H.; Fukuoka, R.; Mouri, M.; Yamamoto, K.; Okamoto, S. Macromolecules 2008, 42, 2115.
10. Sakurai, S. Polymer 2008, 49, 2781.
11. Sakurai, S.; Sakamoto, A.; Itaya, A.; Yamada, K.; Mouri, E.; Matsuoka, H. Int J Appl Chem 2005, 1, 1.
12. Sakurai, S.; Okamoto, S.; Sakurai, K. Developments in Block Copolymer Science and Technology; Hamley, I. W., Ed.; John Wiley & Sons: London, 2004; Chapter 4, p 127.
13. Sasaki, M.; Nakamura, Y.; Fujita, K.; Kinugawa, Y.; Iida, T.; Urahama, Y. J Adhes Sci Technol 2006, 19, 1445.
14. Sasaki, M.; Fujita, K.; Adachi, M.; Fujii, S.; Nakamura, Y.; Urahama, Y. Int J Adhes Adhesives 2008, 28, 372.
15. Nakamura, Y.; Sakai, Y.; Adachi, M.; Fujii, S.; Sasaki, M.; Urahama, Y. J Adhes Sci Technol 2008, 22, 1313.
16. Brandrup, J.; Jmmerjat, E. H., Eds. Polymer Handbook; Wiley: New York, 1989.
17. Gibert, F. X.; Marin, G.; Derail, C.; Allal, A.; Lechat, J. J Adhes 2003, 79, 825.
18. Roos, A.; Creton, C. Macromolecules 2005, 38, 7807.
19. ASTM, D-2979–71, Melt Behaviour of Block Copolymers, pp 127–158.
20. Ueno, S.; Minato, A.; Seto, H.; Amemiya, Y.; Sato, K.; Yamamoto, K.; Okamoto, S.; Nomura, K.; Hara, S.; Akiba, I.; Sakurai, K.; Koyama, A.; Nomura, M.; Sakurai, S. J Phys Chem B 1997, 101, 6847.
21. Nielsen, L. E. Mechanical Properties of Polymers; Reinhold Publishing Corp: New York, 1962.
22. Kim, J. K.; Lee, H. H.; Sakurai, S.; Aida, S.; Masamoto, J.; Nomura, S.; Kitagawa, Y.; Suda, Y. Macromolecules 1999, 32, 6707.
23. Sakurai, S.; Kawada, H.; Hashimoto, T.; Fetters, L. J. Macromolecules 1993, 26, 5796.